

# Chemical Abundances in the Secondary Star of the Black Hole Binary V4641 Sagittarii (SAX J1819.3–2525) \*

Kozo SADAKANE,<sup>1</sup> Akira ARAI,<sup>1</sup> Wako AOKI,<sup>2</sup> Nobuo ARIMOTO,<sup>2</sup> Masahide TAKADA-HIDAI,<sup>3</sup> Takashi OHNISHI,<sup>4</sup>  
Akito TAJITSU,<sup>5</sup> Timothy C. BEERS,<sup>6</sup> Nobuyuki IWAMOTO,<sup>7</sup> Nozomu TOMINAGA,<sup>8</sup> Hideyuki UMEDA,<sup>8</sup>  
Keiichi MAEDA,<sup>9</sup> and Ken'ichi NOMOTO<sup>8</sup>

<sup>1</sup>*Astronomical Institute, Osaka Kyoiku University, Asahigaoka, Kashiwara, Osaka 582-8582*

<sup>2</sup>*National Astronomical Observatory, 2-21-1 Osawa, Mitaka, Tokyo 181-8588*

<sup>3</sup>*Liberal Arts Education Center, Tokai University, 1117 Kitakaname, Hiratsuka, Kanagawa 259-1292*

<sup>4</sup>*Nagoya Science Museum, 2-17-1, Sakae, Naka-ku, Nagoya, Aichi 460-0008*

<sup>5</sup>*Subaru Telescope, National Astronomical Observatory of Japan, 650 North A'ohoku Place,  
Hilo, HI 96720, USA*

<sup>6</sup>*Department of Physics and Astronomy and Joint Institute for Nuclear Astrophysics (JINA),  
Michigan State University, East Lansing, MI 48824, USA*

<sup>7</sup>*Nuclear Data Center, Japan Atomic Energy Agency, Ibaraki 319-1195*

<sup>8</sup>*Department of Astronomy, School of Science, University of Tokyo, Bunkyo-ku, Tokyo 113-0033*

<sup>9</sup>*Department of Earth Science and Astronomy, College of Arts and Sciences, University of Tokyo, Tokyo 153-8902  
sadakane@cc.osaka-kyoiku.ac.jp*

(Received 2006 January 12; accepted 2006 April 12)

## Abstract

We report on detailed spectroscopic studies performed for the secondary star in the black hole binary (micro-quasar) V4641 Sgr in order to examine its surface chemical composition and to see if its surface shows any signature of pollution by ejecta from a supernova explosion. High-resolution spectra of V4641 Sgr observed in the quiescent state in the blue-visual region are compared with those of the two bright well-studied B9 stars (14 Cyg and  $\nu$  Cap) observed with the same instrument. The effective temperature of V4641 Sgr ( $10500 \pm 200$  K) is estimated from the strengths of He I lines, while its rotational velocity,  $v \sin i$  ( $95 \pm 10$  km s<sup>-1</sup>), is estimated from the profile of the Mg II line at 4481 Å. We obtain abundances of 10 elements and find definite over-abundances of N (by 0.8 dex or more) and Na (by 0.8 dex) in V4641 Sgr. From line-by-line comparisons of eight other elements (C, O, Mg, Al, Si, Ti, Cr, and Fe) between V4641 Sgr and the two reference stars, we conclude that there is no apparent difference in the abundances of these elements between V4641 Sgr and the two normal late B-type stars, which have been reported to have solar abundances. An evolutionary model of a massive close binary system has been constructed to explain the abundances observed in V4641 Sgr. The model suggests that the progenitor of the black hole forming supernova was as massive as  $\sim 35M_{\odot}$  on the main-sequence and, after becoming a  $\sim 10M_{\odot}$  He star, underwent "dark" explosion which ejected only N and Na-rich outer layer of the He star without radioactive <sup>56</sup>Ni.

**Key words:** stars:abundances – stars:binaries –stars: individual (V4641 Sagittarii) –stars: micro-quasars –stars: X-rays

## 1. Introduction

The object V4641 Sgr is an X-ray binary with an orbital period of 2.817 d, containing a primary (a black hole) of  $\sim 9.6 M_{\odot}$  and a secondary star of  $5 - 8 M_{\odot}$  (Orosz et al. 2001). Extensive photometric observations were carried out by Goranskij et al. (2003), who reported a photometric period of 2.81728 d, and  $V$  and  $R$  bands light curves which were dominated by ellipsoidal variations from the secondary. They demonstrated that the surface temperature of the secondary is non-uniform from the observed

color variation. They observed a depression in the red wing of the H $\alpha$  line just before the black hole's inferior conjunction, and interpreted this as being due to absorption by the rarefied gas disk around the black hole.

The source exhibited two rapid and bright X-ray flares around 1999 September 15 (Smith et al. 1999). Just prior to the giant X-ray flare, the source showed an increase in the variability (Kato et al. 1999). About six days before the X-ray flare, the source exhibited a  $\sim 1$  mag modulation with a period of  $\sim 2.5$  d. After reaching the peak brightness (8.8 mag in  $V$ ), it decayed rapidly to its mean quiescent level within two days. Since then, the source exhibited several outbursts with very rapid fluctuations in the optical band (Uemura et al. 2002a, 2002b, 2004a,

\* Based on data collected at the Subaru Telescope, which is operated by the National Astronomical Observatory of Japan.

2004b, 2005).

Orosz et al. (2001) carried out extensive spectroscopic observations of V4641 Sgr in 1999 and obtained orbital parameters of the system. The spectral type of the secondary star was assigned to be B9 III. They determined the rotational velocity,  $v \sin i$ , to be  $123 \pm 4 \text{ km s}^{-1}$ , and performed spectroscopic analyses of the secondary star using moderate-resolution spectra to estimate the abundances of several light elements. They found over-abundances of several elements including N, O, Mg, Ca, and Ti, with a solar abundance of Si. Although they note that better data (e.g., high-resolution spectra) or better models are needed before establishing the abundance anomalies, their results on (possible) over-abundances of light elements are very interesting because chemical abundances of the secondary star are expected to provide direct information on the products of nucleosynthesis from supernova explosions of massive stars. Information on abundances is also expected to constrain many physical parameters that are involved in supernova explosion models. They include the mass cut, the amount of fall-back matter, possible mixing, and explosion energies and geometries.

Israelian et al. (1999) reported over-abundances of O, Mg, Si, S, and Ti, but a solar abundance of Fe, in the eclipsing low-mass X-ray binary GRO J1655-40 (Nova Scorpii 1994). Based on this observation and using a variety of supernova models, Podsiadlowski et al. (2002) showed that the best fits can be obtained for He star masses of  $10 - 16 M_{\odot}$ , where spherical hypernova models are generally favored over standard supernova ones. Over-abundances of Al, Ti, and Ni are reported in the black hole binary A0620-00 by González Hernández et al. (2004). They discussed a possible scenario of pollution from a supernova. González Hernández et al. (2005) found enhanced abundances of Ti, Fe, and Ni in the neutron star binary Cen X-4, and showed that these apparent anomalies can be explained if the secondary star captured a significant amount of matter ejected from a spherically symmetric supernova explosion of a  $4 M_{\odot}$  He core progenitor.

In order to clarify the possible abundance anomalies reported in V4641 Sgr, we carried out high-resolution spectroscopic observations using the Subaru telescope and performed comparative abundance analyses using two well-studied reference stars that are reported to have solar abundances.

## 2. Observational Data

Spectroscopic observations of V4641 Sgr were carried out with the Subaru Telescope using the High Dispersion Spectrograph (HDS) on 2005 May 21 and June 19 (UT). Our observations were made during its quiescent state, though the object has been reported to exhibit an outburst on 2005 June 24.371 (UT) (M. Uemura, private communication). Data for two reference stars [14 Cyg = HD 185872 (B9 III) and  $\nu$  Cap = HD193432 (B9.5 V)] were obtained on 2005 May 20 and June 19, respectively, using

the same instrumental setup. Technical details and the performance of the spectrograph are described in Noguchi et al. (2002). We used a slit width of  $1''.0$  (0.5 mm) and a  $2 \times 2$  binning mode, which enabled us to achieve a nominal spectral resolving power of about  $R = 45000$  with a 3.5 pixel sampling. Our observations covered the wavelength region from 4050 Å to 6760 Å with a gap between 5340 – 5450 Å. The exposure times for V4641 Sgr were 4400 sec and 5400 sec on May 21 and June 19, respectively. For flat-fielding of the CCD data, we obtained Halogen lamp exposures (flat images) with the same setup as that for the object frames.

The reduction of two-dimensional echelle spectral data was performed using the IRAF software package in a standard manner. Spectral data extracted from multiple object images of V4641 Sgr were averaged in order to improve the signal-to-noise (S/N) ratio. The wavelength calibration was performed using the Th-Ar comparison spectra obtained during the observations. The measured FWHM of the weak Th lines was  $0.15 \text{ \AA}$  at  $6000 \text{ \AA}$ , and the resulting resolving power was around  $R = 40000$ .

When the observed star shows broadened line profiles due to its high rotational velocity, the process of continuum fitting to the extracted raw spectral data has to be carried out carefully. A very shallow and wide spectral feature might be mistakenly interpreted as the continuum level when a high-order polynomial function is employed in the process. The task of continuum fitting the spectral data for V4641 Sgr was carried out independently by two of us (K. S. and M. T.-H.) using two different approaches. K. S. saved the fitted functions of each echelle order obtained for the spectra of the sharp-lined stars 14 Cyg and  $\nu$  Cap, and used them to divide the raw spectral data of the corresponding echelle orders of V4641 Sgr. Fitted functions of the continuum for 14 Cyg and  $\nu$  Cap were then applied to the V4641 Sgr observations obtained on May 21 and June 20, respectively. M. T.-H. carefully selected line-free windows in each echelle order for spectra of the rapidly rotating spectrophotometric standard star Feige 15 (Takada-Hidai, Aoki, and Zhao 2002), and used them as reference to determine line-free windows in echelle spectra of V4641 Sgr. Since Feige 15 is classified as a spectral type of A0 in the SIMBAD database (which is operated at CDS, Strasbourg, France), its effective temperature can be regarded as being very close to that of V4641 Sgr, with a spectral type of B9 III, suggesting a spectroscopic similarity between the two stars. We found good agreement between the results obtained from the two methods, even for very weak features, and concluded that we had correctly obtained normalized spectral data to be used for the abundance analysis.

We compared the spectra of V4641 Sgr obtained on two nights [May 21 and June 19, at photometric phases 0.38 and 0.62, respectively, which are calculated using data given in Goranskij et al. (2003)] and found no detectable spectral variation. Thus, the data observed on the two nights were averaged in order to obtain the final spectrum, after correcting for the apparent doppler shifts due to the orbital motion. The S/N ratios of the resulting

spectrum of V4641 Sgr were measured at several continuum windows near 5000 Å and 6000 Å. The averaged S/N ratio (per pixel) were around 180 near 5000 Å and 210 near 6000 Å. For the two reference stars, a much higher S/N ratio (around 400) was achieved at 6000 Å.

### 3. Spectral Analysis

An abundance analysis of V4641 Sgr has been carried out relative to the two reference stars 14 Cyg and  $\nu$  Cap. Table 1 lists the absorption lines used in the following analyses. Log  $gf$  values are taken from the VALD database (Kupka et al. 1999); atmospheric parameters ( $T_{\text{eff}}$  and  $\log g$ ) for these two stars were taken from Adelman et al. (2002). They are ( $T_{\text{eff}}$  and  $\log g$ ) = (10750 K, 3.5) and (10250 K, 4.0) for 14 Cyg and  $\nu$  Cap, respectively. Abundance analyses of these two stars have been published in Adelman (1999) (14 Cyg) and in Adelman (1991) ( $\nu$  Cap); solar abundances are reported in these two stars.

We estimated the effective temperature of V4641 Sgr by comparing the strengths of the two He I lines at 4471 Å and 5876 Å in V4641 Sgr and in the two reference stars, as shown in figure 1. In the figure, the observed spectra of these three stars are compared with simulated ones. Spectral simulations were performed using line-blanketed model atmospheres interpolated from Kurucz (1993) and assuming the solar abundances (except for figures 2 and 8, in which an enhanced abundance of Mg by 0.20 dex is assumed). In the spectral simulations, atomic data, except for the major features listed in table 1, are taken from Kurucz and Bell (1995). Equivalent widths of the two He I lines were measured by directly integrating their profiles in the three stars. We found that equivalent widths of both of the He I lines in V4641 Sgr are just around the average of the two reference stars and conclude that the  $T_{\text{eff}}$  of V4641 Sgr is near the average of the two stars ( $10500 \pm 200$  K). This is in agreement with that obtained in Orosz et al. (2001).

We adopt the surface gravity ( $\log g = 3.5$ ) of V4641 Sgr given in Orosz et al. (2001), who obtained this value from the measured widths of the Balmer lines. We use a microturbulent velocity  $\xi_t = 1.6$  km s $^{-1}$  in  $\nu$  Cap (Dworetzky and Budaj 2000), and assume  $\xi_t = 2.0$  km s $^{-1}$  in 14 Cyg. It is difficult to determine the microturbulent velocity in V4641 Sgr because we cannot measure the weak metallic lines, which are in any case unaffected by a change in  $\xi_t$ , in this star. The microturbulent velocity was guessed to be around  $2.5 \pm 0.5$  km s $^{-1}$  by simulating the spectral region between 4505 and 4535 Å, where moderately strong (80 - 150 mÅ) Fe II lines can be found, to obtain the best fitting, assuming an appropriate rotational velocity ( $v \sin i$ , described in the next section).

### 4. Results

We estimate the rotational velocity,  $v \sin i$ , of V4641 Sgr from the observed profile of the Mg II line at 4481 Å, as shown in figure 2. First, we tried to reproduce the

profiles of the line in 14 Cyg and  $\nu$  Cap by adopting the mean values of published data of  $v \sin i$ . They are 30 and 25 km s $^{-1}$  for 14 Cyg (Abt and Morrell 1995; Royer et al. 2002) and  $\nu$  Cap (Abt et al. 2002; Dworetzky and Budaj 2000; Fekel 2003; Royer et al. 2002), respectively. We find that acceptable reproductions of the observed line profile can be obtained using adopted values of  $v \sin i$  for the two stars, as shown in figure 8. Next, we searched for a suitable value of  $v \sin i$  in V4641 Sgr by exploring values between 60 and 150 km s $^{-1}$ ; we found that the best fit is achieved at  $95 \pm 10$  km s $^{-1}$ . If we use  $v \sin i = 123$  km s $^{-1}$ , as obtained in Orosz et al. (2001), the simulated profile becomes too shallow and too wide (figure 2). We conclude that their result of  $v \sin i$  is too large, most probably resulting from the low resolution of their spectral data.

We tried to estimate the abundance of C in V4641 Sgr using the C II line at 4267 Å (figure 3). The line consists of two major components at 4267.001 Å and at 4267.261 Å (table 2). The C II feature in  $\nu$  Cap can be reproduced with a solar abundance of C, while the observed feature in 14 Cyg appears to be too weak. This may suggest either a slight under-abundance of C or an error in the adopted atmospheric parameters for 14 Cyg. We find that the broad feature at 4267 Å in V4641 Sgr can be reproduced by assuming a solar abundance of C.

We find a shallow and broad absorption feature at 6483 Å in V4641 Sgr in both the May 20 and June 19 data. Comparisons with the two reference stars (figure 4) shows that the feature in V4641 Sgr appears to be too deep. The feature coincides with the positions of the five components of N I lines (Multiplet No. 21). We simulated spectra of both reference stars, assuming solar abundances, and find that observations can be reasonably reproduced when excluding the sharp components due to atmospheric absorption. The only observable feature is the Fe II line at 6482.204 Å. On the other hand, the observed feature of V4641 Sgr at 6483 Å cannot be reproduced when we assume solar abundances of N and Fe. A reasonable reproduction can be obtained when a significant over-abundance of N (by around 1.0 dex) is assumed, as shown in figure 4. Allowing for a slight uncertainty in the continuum level because of the low S/N ratio, we conclude that N is indeed over-abundant in V4641 Sgr by at least 0.8 dex. This conclusion is in accordance with the result noted in Orosz et al. (2001), who obtained an over-abundance of N by 1.0 dex from an analysis of the same spectral feature.

Analyses of weak O I lines near 6455 Å are shown in figure 5. We conclude that the O I feature can be reasonably fit by using a solar O abundance. This is in contrast with the result given in Orosz et al. (2001), who obtained an over-abundance of O (by a factor of three), when analysing the same spectral feature.

Next, we analyse the Na I D lines. The D lines are usually contaminated by interstellar absorption superposed on the stellar components, as shown for 14 Cyg and  $\nu$  Cap (figure 6). Fortunately, spectral lines of V4641 Sgr observed on July 19 are significantly redshifted (by +210

km s<sup>-1</sup>), and we can analyse both of the D1 and D2 components, which are unaffected by interstellar absorptions. The broad D lines in V4641 Sgr are too strong to be accounted for by the solar Na abundance. As is shown in figure 6, we need to enhance the abundance of Na by 0.7 dex in order to fit the D2 line. Further enhancement (by 0.2 dex) of the Na abundance is needed to fit the D1 line (although the D1 line is heavily affected by atmospheric absorption). Upon averaging the results obtained from the D1 and D2 lines, we concluded that Na is over-abundant by at least 0.8 dex in V4641 Sgr.

The abundances of six elements (Mg, Si, Al, Ti, Cr, and Fe) in V4641 Sgr were estimated by comparing the major absorption features of each element with those seen in the two reference stars. figures 7 to 11 display the results. In these figures, the solid lines show simulated spectra for each star, assuming solar abundances (except for figure 8, where an enhanced abundance of Mg is assumed), taken from Grevesse and Sauval (1998). Neutral and singly ionized lines of Mg are shown in figures 7 and 8, respectively. We find that the Mg I triplet lines can be reproduced with a solar abundance of Mg, while a slight enhancement (0.20 dex) of Mg is suggested from the observed profile of the Mg II line at 4481 Å. On the other hand, the Mg II feature at 4390.5 Å in V4641 Sgr can be reproduced by assuming a solar Mg abundance. Thus, we conclude that the abundance of Mg in V4641 Sgr coincides with that of the Sun, which differs from the results reported by Orosz et al. (2001), who concluded that this star exhibits an enhanced (by a factor of seven) abundance of Mg.

We find that an Al II line at 4663.05 Å is clearly present in both of the two reference stars, and in V4641 Sgr (figure 9). Our spectral analyses of this line suggests that Al may be slightly over-abundant (by +0.2 dex) in V4641 Sgr, although the relatively poor S/N ratio in the blue region does not allow for a reliable analysis of the line. A pair of Si II lines near 5050 Å are compared in figure 10. We conclude that the abundance of Si in V4641 Sgr is close to the solar abundance. In figure 11, we compare Ti II, Cr II, and Fe II lines, where all of the absorption features can be reproduced by assuming the same (solar) abundances in the three stars. We analyse several other strong Ti II, Cr II, and Fe II lines (noted in table 1) and found that all of these features in V4641 Sgr can be explained using solar abundances of Ti, Cr, and Fe. Our result for Ti is again in contrast with the result given in Orosz et al. (2001), who obtained an over-abundance of Ti (by a factor of 10). They used four Ti II lines (at 5129.2 Å, 5185.9 Å, 5188.7 Å, and at 5226.5 Å) to obtain the Ti abundance, and pointed out a high abundance of Ti from the two lines (at 5129.2 Å and 5226.5 Å) using data of spectral resolution of about 4 Å. We examined all of these lines on our high-resolution data and find that all these lines are very weak in the reference stars, and also in V4641 Sgr, when compared to those Ti II lines listed in table 1. We concluded that the four lines used in Orosz et al. (2001) are inadequate to be used for the abundance analysis of Ti.

Our final derived abundances for 10 observed elements

(11 ions) are summarized in table 2, together with their expected errors. We estimate uncertainties in the abundances of each ion introduced by errors in the adopted parameters: 200 K in  $T_{\text{eff}}$ , 0.5 in  $\log g$ , and 0.5 km s<sup>-1</sup> in  $\xi_t$ . When these errors are combined, we conclude that the our abundance analysis results are reliable within 0.25 dex (table 2). We examined the effect of a difference in spectral resolution on the resulting abundances by a simple test. The original data of both 14 Cyg and V4641 Sgr were degraded to around  $R = 8000$ , the highest resolution used in Orosz et al. (2001), by convolving with an appropriate Gaussian function. We then repeated abundance analyses using the degraded data for several spectral features such as the Mg II line at 4481 Å, the Mg I triplet lines, and the three Ti II lines listed in table 1. Fairly good agreements (within 0.05 dex) were found for 14 Cyg from both high and low resolution data. On the other hand, differences as large as 0.15 dex were found between abundance results obtained from weak and noisy spectral features in the case of V4641 Sgr. We infer that these differences are mainly resulted from the relatively poor SN ratio in the V4641 Sgr data, but not from the difference in the spectral resolution. When the limited S/N ratio of our observation and the high rotational velocity of V4641 Sgr are taken into account, the expected error in the abundances should be increased to around 0.3 dex.

## 5. Discussion

We obtained abundances of 10 elements in V4641 Sgr, and found definite over-abundances of only two elements (N and Na). The abundances of the eight other elements in V4641 Sgr have been shown to be the same as those in the two reference stars (solar abundances), except for a possible enhancement of Mg suggested from the Mg II line at 4481 Å and that of Al. However, when averaged with the result obtained from the Mg I triplet lines and the Mg II line at 4390.5 Å, the abundance of Mg is coincident with that in the reference stars within the expected error ( $[\text{Mg}/\text{H}] = +0.10 \pm 0.30$ ). The above conclusions are in contrast to the results noted in Orosz et al. (2001) except for N, where they concluded over-abundances of N (1.0 dex), O (0.48 dex), Mg (0.85 dex), and Ti (1.0 dex) in V4641 Sgr when compared to the Sun. We suggest that the primary reason for obtaining discordant abundances for O, Mg, and Ti is the difference in the spectral resolution of the data. Orosz et al. (2001) used a much lower resolving power ( $R$  ranging from 1200 to 7700) than obtained in the present study ( $R \sim 40000$ ).

Our results for the abundances of the light elements in the secondary star of V4641 Sgr [definite over-abundances of N and Na, normal (solar) abundances of O, and the  $\alpha$ -elements Mg, Si, and Ti] are unique when compared with the results obtained for other X-ray binaries. Abundances obtained in four secondary stars in X-ray binaries are compared in figure 12 [V4641 Sgr (this study), GRO J1655-40 (Israeli et al. 1999), A0620-00 (González Hernández et al. 2004), and Cen X4 (González Hernández et al. 2005)]. We note that all four stars show distinct abundance pat-

terns. The  $\alpha$ -elements (O, Mg, Si, S, and Ti) are definitely over-abundant in GRO J1655-40, while they appear to be normal in V4641 Sgr. Fe is over-abundant only in Cen X-4. N and Na are over-abundant only in V4641 Sgr. The difference in the abundances of O between V4641 Sgr and GRO J1655-40 is impressive. The observed abundance pattern in V4641 Sgr (enhanced N and Na, and normal  $\alpha$ -elements) seems to be different from those of the usual supernova models that predict the enhancement of  $\alpha$ -elements (Podsiadlowski et al. 2002, González Hernández et al. 2004, and González Hernández et al. 2005). However, these variations of abundance patterns can be explained with the variations of the abundances of supernova explosions that are associated with black hole formation (Umeda and Nomoto 2003).

In order to explain the abundances in V4641 Sgr quantitatively, we calculated the evolution of the star with the initial mass of  $40 M_{\odot}$  and the solar metallicity from the main-sequence to collapse as in Umeda and Nomoto (2005) and constructed the following evolutionary models for V4641 Sgr. In the close binary system, this  $40 M_{\odot}$  primary star underwent a common envelope phase and lost most of its H-rich envelope until it became a He star of mass  $15.14 M_{\odot}$ . The system also lost its angular momentum and became compact with the orbital period as short as that observed. Figure 13 shows the abundance distribution near the surface of the He star at the onset of collapse. In the He-rich layer,  $^{14}\text{N}$  and  $^{23}\text{Na}$  were enhanced by the CNO-cycle and Ne-Na cycle (proton captures on  $^{21}\text{Ne}$  and  $^{22}\text{Ne}$ ) during H-burning. In the deeper He layer, the  $^{14}\text{N}$  abundance was decreased by successive  $\alpha$ -capture to produce  $^{22}\text{Ne}$  during weak He shell burning.

The  $15 M_{\odot}$  He star is massive enough to eventually formed a black hole (BH). We assume that the collapse induced a relatively weak explosion. Generally, an explosion with a smaller energy leads to a larger amount of fall back materials and thus a smaller amount of ejecta (e.g., Iwamoto et al. 2005). In order to reproduce the observations of V4641 Sgr, we assume that the kinetic energy of explosion was as small as  $E = 6 \times 10^{49}$  ergs. In such a weak explosion, only  $0.5 M_{\odot}$  materials above  $M_r = 14.66 M_{\odot}$  were ejected. The abundance distribution in the He layer in figure 13 does not change in the explosion. A part of the ejected materials must be captured by the secondary star. The captured (accreted) materials were then mixed with the materials of solar metallicity in the atmosphere of the secondary star. Since the ejecta is relatively N- and Na-rich without any enhancement of  $\alpha$ -elements, this could explain the observed abundance pattern of V4641 Sgr. If the accreted material is mixed with 40-times larger amount of secondary star materials, the final abundance pattern would be consistent with the observed abundance pattern of the secondary star (figure 14). Here, most of the heavy elements above Na originated from the materials of V1641 Sgr. Such a partial mixing (e.g., slow rotational mixing) may be realized because the surface temperature of V4641 Sgr is too high for deep convective mixing to occur.

We should note that an alternative scenario is possi-

ble. If the stellar wind of the He star of  $\sim 15 M_{\odot}$  blows at a high enough rate, a part of the N- and Na-rich materials in the He layer would have been blown off and captured by the secondary star. If the energy of supernova explosion was even smaller than  $\sim 6 \times 10^{49}$ , no mass ejection occurred. These processes could lead to the observed abundance pattern of V4641 Sgr. The above  $40 M_{\odot}$  model formed a BH of  $14 M_{\odot}$ . The initially  $30 M_{\odot}$  model produces a similar abundance pattern by forming a  $7.2 M_{\odot}$  BH. Since the observed BH mass of V4641 Sgr is  $\sim 9.6 M_{\odot}$ , the progenitor of the BH in V4641 is likely a  $\sim 35 M_{\odot}$  star. It is highly uncertain in the current supernova models under what condition the BH formation can induce a supernova explosion and how much explosion energy can be released; it may depend on the rotation of the BH and the progenitor. The case of V4641 Sgr suggests the BH-forming supernova was really *dark*, because no radioactive  $^{56}\text{Ni}$  was ejected. Such a *dark* supernova corresponds to the extreme end of the *faint* supernova branch (Nomoto et al. 2005).

Another possible scenario is the contamination by rotationally induced mixing in the secondary star, itself. However, the observed rotational velocity ( $v \sin i \sim 100 \text{ km s}^{-1}$ ) and estimated mass may be lower than those predicted for the simultaneous enhancements of N and Na, although they strongly depend on the uncertain inclination.

We thank Drs. K. Matsumoto and M. Uemura for comments and suggestions. This research was partly supported by Grants-in-Aid from the Ministry of Education, Culture, Sports, Science and Technology (No. 15540236 KS, No. 17540218 MTH, No. 17740163 NI, and No. 17033002 KN). T.C.B. acknowledges partial support from grant AST 04-06784, as well as from grant PHY 02-16783, Physics Frontier Center/Joint Institute for Nuclear Astrophysics (JINA), awarded by the US National Science Foundation.

## References

- Abt, H. A., Levato, H., & Grosso, M. 2002, ApJ, 573, 359
- Abt, H. A., & Morrell, N. I. 1995, ApJS, 99, 135
- Adelman, S. J. 1991, MNRAS, 252, 116
- Adelman, S. J. 1999, MNRAS, 310, 146
- Adelman, S. J., Pintado, O. I., Nieva, F., Rayle, K. E., & Sanders, S. E., Jr. 2002, A&A, 392, 1031
- Dworetzky, M. M., & Budaj, J. 2000, MNRAS, 318, 1264
- Fekel, F. C. 2003, PASP, 115, 807
- González Hernández, J. I., Rebolo, R., Israelian G., & Casares, J. 2004, ApJ, 609, 988
- González Hernández, J. I., Rebolo, R., Israelian G., Casares, J., Maeda, K., Bonifacio, P., & Molaro, P. 2005, ApJ, 630, 495
- Goranskij, V. P., Barsukova, E. A., & Burenkov, A. N. 2003, Astronomy Rept., 47, 740
- Grevesse, N., & Sauval, A. J. 1998, Space Sci. Rev., 85, 161
- Israelian, G., Rebolo, R., Basri, G., Casares, J., & Martin, E. L. 1999, Nature, 401, 142

- Iwamoto, N., Umeda, H., Tominaga, N., Nomoto, K., & Maeda, K. 2005, *Science*, 309, 451
- Kato, T., Uemura, M., Stubbings, R., Watanabe, T., & Monard, B. 1999, *Inf. Bull. Variable Stars*, 4777
- Kupka, F., Piskunov, N., Ryabchikova, T. A., Stempels, H.C., & Weiss, W.W. 1999, *A&AS*, 138, 119
- Kurucz, R. L. 1993, Kurucz CD-ROM, No.13 (Harvard-Smithsonian Center for Astrophysics)
- Kurucz, R. L., & Bell, B. 1995, Kurucz CD-ROM, No.23 (Harvard-Smithsonian Center for Astrophysics)
- Noguchi, K., et al. 2002, *PASJ*, 54, 855
- Nomoto, K., Tominaga, N., Umeda, H., Maeda, K., Ohkubo, T., & Deng, J. 2005, *Nuclear Phys.*, A 758, 263c
- Orosz, J. A., et al. 2001, *ApJ*, 555, 489
- Podsiadlowski, P., Nomoto, K., Maeda, K., Nakamura, T., Mazzali, P., & Schmidt, B. 2002, *ApJ*, 567, 491
- Royer, F., Grenier, S., Baylac, M. -O., Gomez, A. E., & Zorec, J. 2002, *A&A*, 393, 897
- Smith, D. A., Levine, A. M., & Morgan, E. H., 1999, *IAU Circ.*, 7253, 2
- Takada-Hidai, M., Aoki, W., & Zhao, G. 2002, *PASJ*, 54, 899
- Uemura, M., et al. 2002a, *PASJ*, 54, 95
- Uemura, M., et al. 2002b, *PASJ*, 54, L79
- Uemura, M., et al. 2004a, *PASJ*, 56, S61
- Uemura, M., et al. 2004b, *PASJ*, 56, 823
- Uemura, M., et al. 2005, *Inf. Bull. Variable Stars*, 5626
- Umeda, H., & Nomoto, K. 2003, *Nature*, 422, 871
- Umeda, H., & Nomoto, K. 2005, *ApJ*, 619, 427

**Table 1.** Lines used in abundance analyses.

	Wavelength(Å)	$\chi$ (eV)	$\log gf$
He I	4471.469	20.964	-2.198
	4471.473	20.964	-1.028
	4471.473	20.964	-0.278
	4471.485	20.964	-1.028
	4471.488	20.964	-0.548
	4471.682	20.964	-0.898
	5875.599	20.964	-1.511
	5875.614	20.964	-0.341
	5875.615	20.964	0.409
	5875.625	20.964	-0.341
	5875.640	20.964	0.139
5875.966	20.964	-0.211	
C II	4267.001	18.046	0.562
	4267.261	18.046	-0.584
	4267.261	18.046	0.717
	4267.261	18.046	-0.584
N I	6480.512	11.753	-1.420
	6481.706	11.750	-1.063
	6482.699	11.764	-0.510
	6483.753	11.753	-0.857
O I	6484.808	11.758	-0.674
	6453.602	10.740	-1.288
	6454.444	10.740	-1.066
	6455.977	10.741	-0.920
Na I	5889.951	0.00	0.117
	5895.924	0.00	-0.184
Mg I	5167.321	2.709	-1.030
	5172.684	2.712	-0.402
	5183.604	2.717	-0.180
Mg II	4390.514	9.99	-1.490
	4390.572	9.99	-0.530
	4481.126	8.864	0.740
	4481.325	8.864	0.590
Al II	4663.046	10.598	-0.284
	5041.024	10.067	0.291
Si II	5055.984	10.074	0.593
	5056.317	10.074	-0.359
	4395.000	1.084	-0.510
Ti II	4501.270	1.116	-0.760
	4571.960	1.572	-0.230
	4558.660	4.073	-0.449
Cr II	4588.220	4.071	-0.627
	4592.070	4.074	-1.221
	4508.280	2.856	-2.250
Fe II	4515.340	2.844	-2.450
	4576.330	2.844	-2.920
	4582.840	2.844	-3.090
	4583.830	2.807	-1.860
	4629.340	2.807	-2.330

**Table 2.** Abundances in V4641 Sgr.

	C II	N I	O I	Na I	Mg I	Mg II	Al II	Si II	Ti II	Cr II	Fe II
[X/H]	0.0	+0.8	0.0	+0.8	0.0	+0.1	+0.2	0.0	0.0	0.0	0.0
Error(A)	0.12	0.02	0.01	0.12	0.13	0.03	0.04	0.03	0.10	0.05	0.04
Error(B)	0.27	0.0	0.01	0.16	0.18	0.19	0.14	0.06	0.03	0.10	0.13
Error(C)	0.01	0.02	0.0	0.13	0.10	0.02	0.08	0.05	0.13	0.09	0.10

Note. — [X/H]: logarithmic abundances relative to the Sun; Error (A), (B), and (C): expected uncertainties in the abundance introduced by errors in  $T_{\text{eff}}$  (200 K),  $\log g$  (0.5), and in  $\xi_t$  (0.5 km s<sup>-1</sup>), respectively.

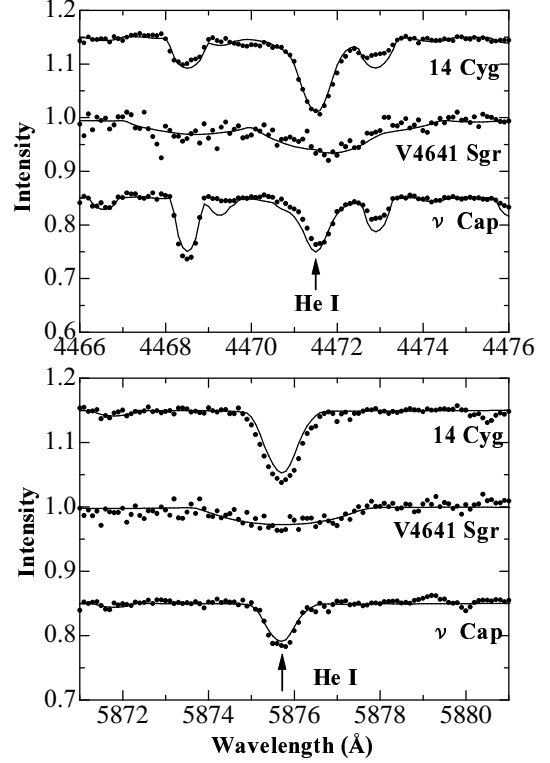


**Fig. 1.** Comparisons of He I lines. Profiles of two He I lines at 4471 Å and at 5876 Å in V4641 Sgr and in two comparison stars 14 Cyg and in  $\nu$  Cap are compared in the upper and lower panels, respectively. The dots and solid lines show the observation and the simulated spectra calculated assuming the solar abundances, respectively. Rotational velocities,  $v \sin i$ , of 30, 25, and 95 km s<sup>-1</sup> are used for 14 Cyg,  $\nu$  Cap, and V 4641 Sgr, respectively.

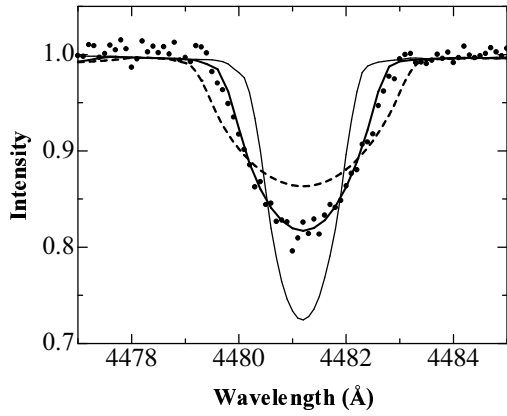


**Fig. 2.** Rotational velocity,  $v \sin i$ , of V4641 Sgr. A small section of the observed spectrum near the Mg II line at 4481.2 Å is shown by dots. Simulated spectra, calculated assuming the abundance of Mg,  $[\text{Mg}/\text{H}] = 0.2$ , for  $v \sin i = 130, 95$ , and  $60 \text{ km s}^{-1}$  are shown by dashed, thick solid, and thin solid lines, respectively.

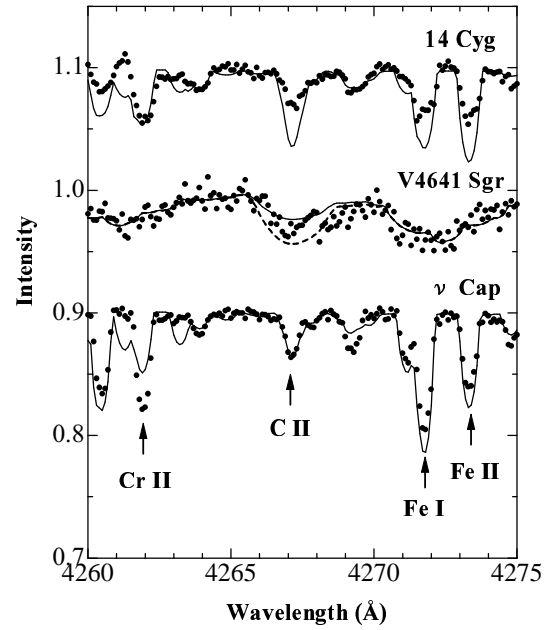


**Fig. 3.** Analysis of the C II feature at 4267.2 Å. The dots and thin solid lines show the observation and the simulated spectra calculated assuming the solar abundances of C. The thick dashed line (for V4641 Sgr) show the case when C is over-abundant by 0.7 dex.

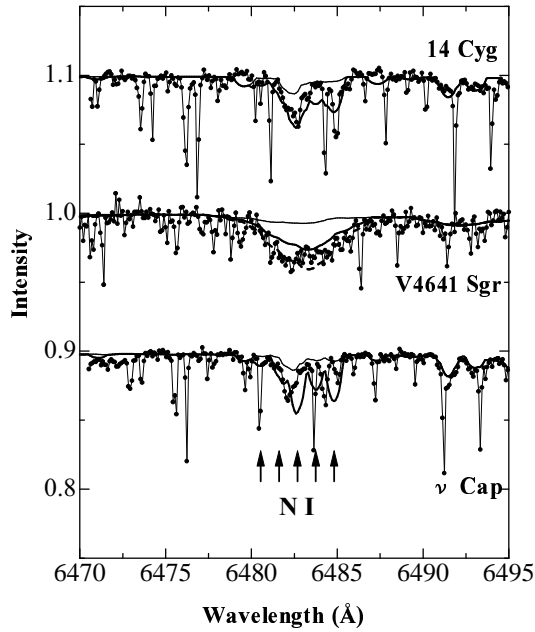


**Fig. 4.** Analysis of the N I feature near 6483 Å. The dots and thin solid lines show the observation and the simulated spectra calculated assuming the solar abundances of N. Many sharp absorption features are caused by atmospheric H<sub>2</sub>O molecules. The thick solid lines and the dashed line (for V4641 Sgr) show the case when N is over-abundant by 1.0 dex and 1.5 dex, respectively.

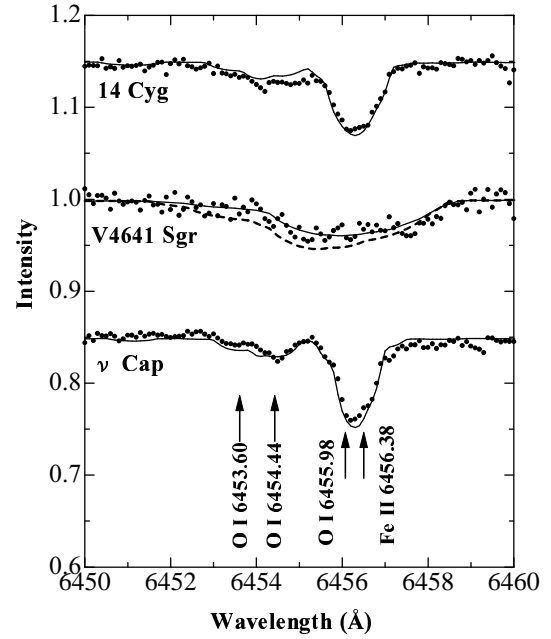


**Fig. 5.** Analysis of O I lines near 6455 Å. The dots and solid lines show the observation and the simulated spectra calculated assuming solar abundances of O and Fe, respectively. The dashed line for V4641 Sgr is the case when O is 0.5 dex over-abundant as noted in Orosz et al. (2001).

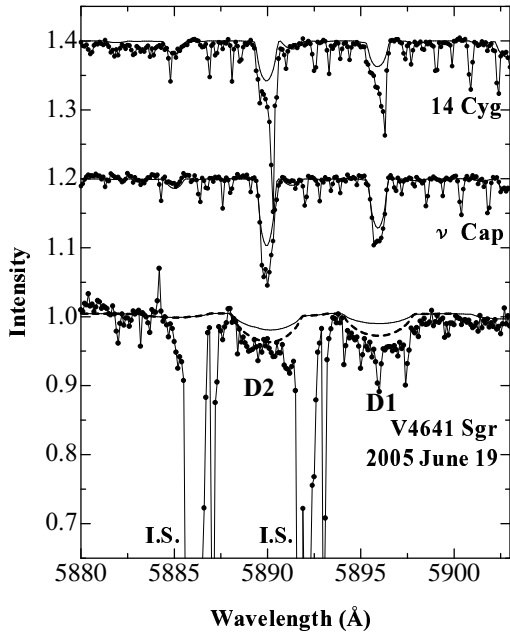


**Fig. 6.** Analysis of the Na I D lines. Both D1 and D2 lines in 14 Cyg and  $\nu$  Cap are contaminated by sharp interstellar (I.S.) components. The I.S. lines of V4641 Sgr observed on 2005 June 19 are apparently blue-shifted by  $210 \text{ km s}^{-1}$  due to the orbital motion of the star. The dots and thin solid lines show the observation and the simulated spectra calculated assuming the solar abundances of Na. The dashed line for V4641 Sgr shows the case when Na is over-abundant by 0.7 dex.

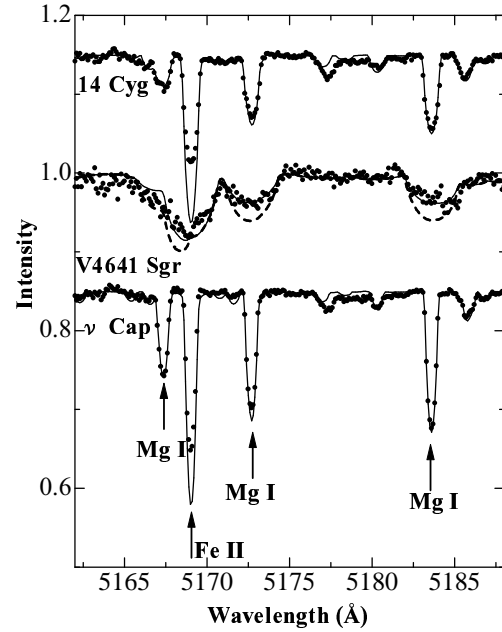


**Fig. 7.** Analysis of the Mg I triplet lines. Dots and solid lines show the observation and the simulated spectra calculated assuming solar abundances of Mg and Fe, respectively. The dashed line for V4641 Sgr is the case when Mg is 0.85 dex over-abundant as noted in Orosz et al. (2001).

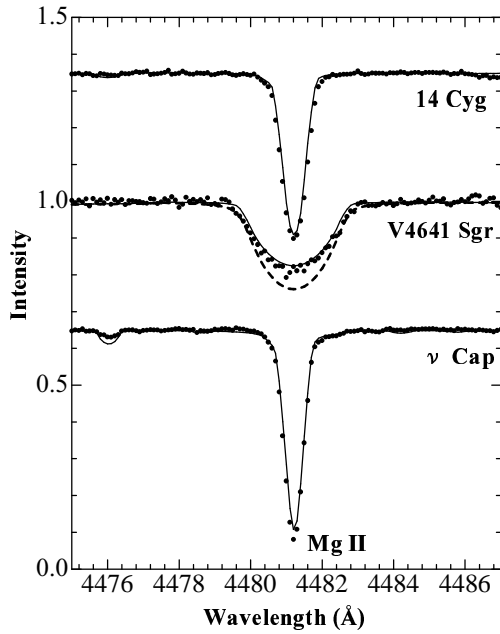


**Fig. 8.** Analysis of the Mg II line at 4481 Å. The dots represent observed spectra. The solid lines for 14 Cyg and  $\nu$  Cap are simulated spectra calculated assuming the solar abundance of Mg, while that for V4641 Sgr is calculated assuming an enhanced (by 0.20 dex) abundance of Mg. The dashed line for V4641 Sgr is the case when Mg is 0.85 dex over-abundant as noted in Orosz et al. (2001).

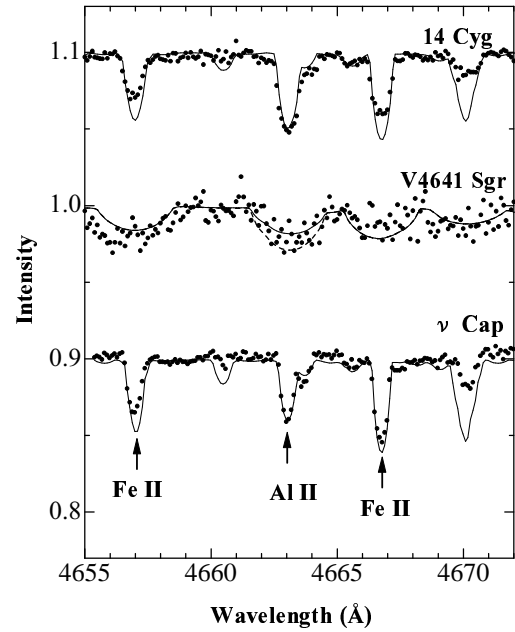


**Fig. 9.** Analysis of the Al II line at 4663 Å. The dots and solid lines show the observation and the simulated spectra calculated assuming a solar abundances for Al, respectively. The dashed line for V4641 Sgr is the case when Al is 0.5 dex over-abundant.

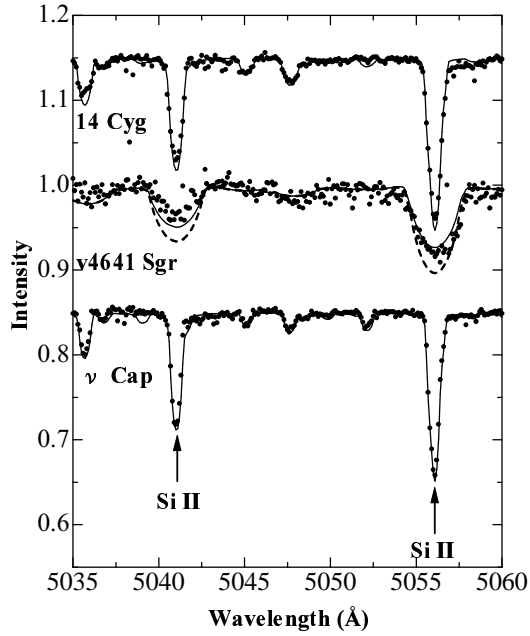


**Fig. 10.** Analysis of a pair of Si II lines near 5050 Å. The dots and solid lines show the observation and the simulated spectra calculated assuming the solar abundance of Si, respectively. The dashed line for V4641 Sgr is the case when Si is 0.5 dex over-abundant.

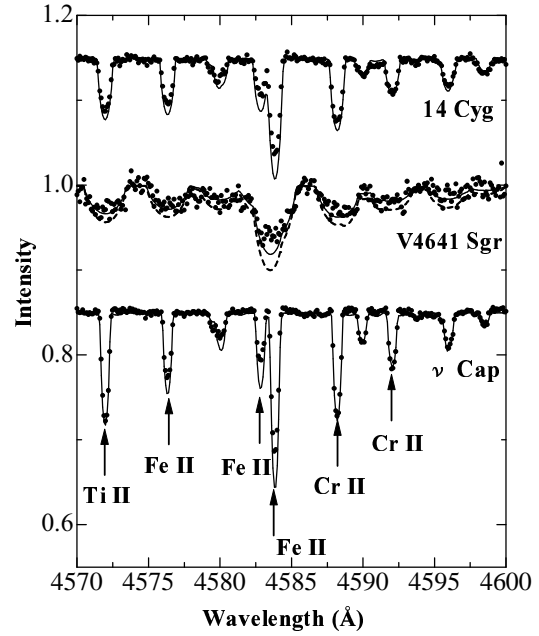


**Fig. 11.** Analysis of Ti II, Cr II, and Fe II lines near 4585 Å. The dots and solid lines show the observation and the simulated spectra calculated assuming solar abundances of Ti, Cr, and Fe, respectively. The dashed line for V4641 Sgr is the case when Ti, Cr, and Fe are 0.2 dex over-abundant.

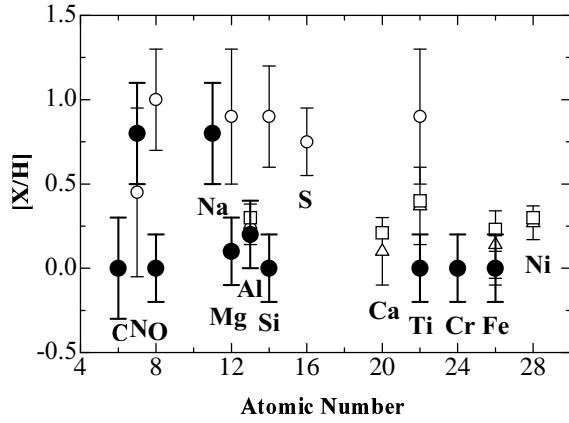


**Fig. 12.** Comparison of metal abundances.  $[X/H]$  values, logarithmic abundance of the element X relative to the Sun, in four secondary stars are plotted against the atomic number. Filled circles, open circles, open triangles, and open squares are for V4641 Sgr, GRO J1655-40, A0620-00, and for Cen X-4, respectively.

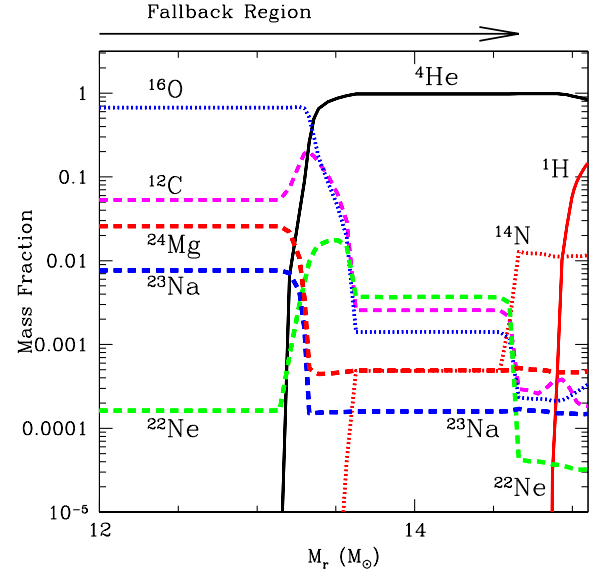


**Fig. 13.** Internal abundance distribution of the solar metallicity  $15.14M_{\odot}$  He star model at the onset of collapse. This He star is the core of the  $40M_{\odot}$  star. The extent of the large scale fallback is  $M_r = 14.66M_{\odot}$  shown by right-headed arrow. The remaining black hole mass is  $14.66M_{\odot}$ . The main contribution for Na as well as for N comes from H-burning. N and Na abundances in the He layers are enhanced with respect to the initial abundances of  $1.2 \times 10^{-3}$  and  $3.5 \times 10^{-5}$ , respectively.

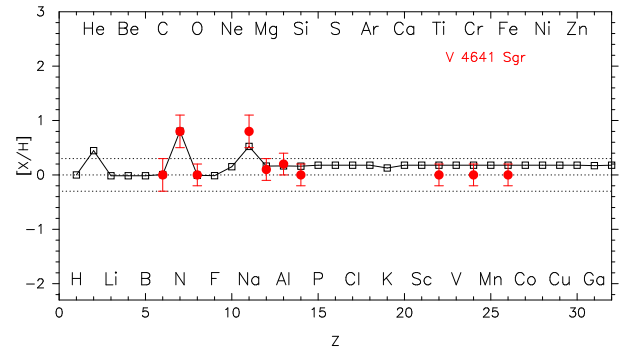


**Fig. 14.** Comparison of V4641 Sgr with a mixture of the solar metallicity  $15.14M_{\odot}$  He star supernova ejecta and the secondary star materials. The assumed ratio of the supernova ejecta to the secondary star materials is 1/40. The filled circles with error-bars show the observed abundances. The abundance pattern of the mixture is represented by open squares connected with solid lines. The yield shows that, except for the enhancements of N and Na, all the other elements have almost solar ratios. Black hole with the mass of  $14.66M_{\odot}$  is left behind.